RESEARCH ARTICLE | *Control of Coordinated Movements*

Compensating for intersegmental dynamics across the shoulder, elbow, and wrist joints during feedforward and feedback control

Rodrigo S. Maeda,[1,2,3] **Tyler Cluff,**[5,6] **Paul L. Gribble,**[1,3,4] **and J. Andrew Pruszynski**[1,2,3,4,7]

[1]*Brain and Mind Institute, Western University, London, Ontario, Canada;* [2]*Robarts Research Institute, Western University, London, Ontario, Canada;* [3]*Department of Psychology, Western University, London, Ontario, Canada;* [4]*Department of Physiology and Pharmacology, Western University, London, Ontario, Canada;* [5]*Faculty of Kinesiology, University of Calgary, Calgary, Alberta, Canada;* [6]*Hotchkiss Brain Institute, University of Calgary, Calgary, Alberta, Canada; and* [7]*Department of Integrative Medical Biology, Umea University, Umea, Sweden*

Maeda RS, Cluff T, Gribble PL, Pruszynski JA. Compensating for intersegmental dynamics across the shoulder, elbow, and wrist joints during feedforward and feedback control. *J Neurophysiol* 118: 1984–1997, 2017. First published July 12, 2017; doi:10.1152/jn.00178.2017.—Moving the arm is complicated by mechanical interactions that arise between limb segments. Such intersegmental dynamics cause torques applied at one joint to produce movement at multiple joints, and in turn, the only way to create single joint movement is by applying torques at multiple joints. We investigated whether the nervous system accounts for intersegmental limb dynamics across the shoulder, elbow, and wrist joints during self-initiated planar reaching and when countering external mechanical perturbations. Our first experiment tested whether the timing and amplitude of shoulder muscle activity account for interaction torques produced during single-joint elbow movements from different elbow initial orientations and over a range of movement speeds. We found that shoulder muscle activity reliably preceded movement onset and elbow agonist activity, and was scaled to compensate for the magnitude of interaction torques arising because of forearm rotation. Our second experiment tested whether elbow muscles compensate for interaction torques introduced by single-joint wrist movements. We found that elbow muscle activity preceded movement onset and wrist agonist muscle activity, and thus the nervous system predicted interaction torques arising because of hand rotation. Our third and fourth experiments tested whether shoulder muscles compensate for interaction torques introduced by different hand orientations during self-initiated elbow movements and to counter mechanical perturbations that caused pure elbow motion. We found that the nervous system predicted the amplitude and direction of interaction torques, appropriately scaling the amplitude of shoulder muscle activity during self-initiated elbow movements and rapid feedback control. Taken together, our results demonstrate that the nervous system robustly accounts for intersegmental dynamics and that the process is similar across the proximal to distal musculature of the arm as well as between feedforward (i.e., self-initiated) and feedback (i.e., reflexive) control.

NEW & NOTEWORTHY Intersegmental dynamics complicate the mapping between applied joint torques and the resulting joint motions. We provide evidence that the nervous system robustly predicts these intersegmental limb dynamics across the shoulder, elbow, and wrist joints during reaching and when countering external perturbations.

MOST ARM MOVEMENTS require the nervous system to coordinate multiple joints. Complicating this coordination are mechanical interactions between limb segments that arise because torques generated at one joint cause rotational forces at other joints, and thus produce motions without muscle contraction (Hollerbach and Flash 1982). For a two-link arm in the horizontal plane, for example, applying torque only at the elbow will cause both the shoulder and elbow to move. Thus the only way to produce a single-joint elbow movement is to generate torque at both the shoulder and elbow joints.

Many researchers have examined how the nervous system accounts for the arm's intersegmental dynamics during feedforward (i.e., self-initiated) reaching movements (Almeida et al. 1995; Cooke and Virji-Babul 1995; Corcos et al. 1989; Galloway and Koshland 2002; Gottlieb 1998; Gribble and Ostry 1999; Gritsenko et al. 2011; Hollerbach and Flash 1982; Koshland et al. 1991; Pigeon et al. 2003, 2013; Sainburg et al. 1995, 1999; Virji-Babul and Cooke 1995). As a whole, these studies clearly indicate that control signals sent to arm muscles appropriately predict upcoming interaction torques and thus likely rely on an internal model of mechanical interactions between limb segments (Wolpert and Flanagan 2001). For example, in the context of both constrained and unconstrained single-joint movements, Almeida et al. (1995) demonstrated that muscle activation patterns at a stationary joint (either the shoulder or elbow) counteract the interaction torques that arise because of the motion of the adjacent joint and thus prevent their movement. Gribble and Ostry (1999) further showed that shoulder muscle activity predictively accounts for interaction torques by showing that shoulder muscle activity occurs before movement onset and scales appropriately with differences in the speed and amplitude of single-joint elbow movements.

The loss of somatosensory feedback impairs the nervous system's ability to account for the mechanical interactions between limb segments (Sainburg et al. 1995, 1999). Indeed,

several groups have investigated whether rapid feedback responses (i.e., reflexes) are modulated in a way that accounts for these mechanical interactions (Crevecoeur et al. 2012; Kurtzer et al. 2008, 2009, 2014, 2016; Lacquaniti and Soechting 1984, 1986a, 1986b; Pruszynski et al. 2011; Soechting and Lacquaniti 1988). For example, Kurtzer et al. (2008) applied a combination of shoulder and elbow torque perturbations that led to minimal shoulder motion but different amounts of elbow motions. This approach allowed them to test whether rapid feedback responses in shoulder muscles were dependent on local stretch information or whether they accounted for the limb's dynamics and thus responded to the applied torques. Their results showed that the short-latency feedback response (20–50 ms postperturbation), which is mediated by spinal circuits, responded only to local joint motion. In contrast, the long-latency feedback response (50–100 ms postperturbation), which is partially mediated by the same cortical structures that contribute to self-initiated reaching (Pruszynski and Scott 2012; Shemmell et al. 2010), responded to the underlying applied torques. This is consistent with the idea that long-latency responses are organized on the basis of an internal model of intersegmental dynamics.

Although these previous studies are consistent with the idea that both voluntary and feedback control of the arm make use of an internal model of the limb's dynamics, the investigations have typically focused on a limited set of parameters in the context of two joints, usually the shoulder and elbow (but see Pigeon et al. 2003). In the present study, we performed four experiments with a three-degree-of-freedom exoskeleton robot that allows flexion and extension movements of the shoulder, elbow, and wrist joints. The main goal of these experiments was to examine how robustly the nervous system accounts for intersegmental dynamics across these three joints. In our first experiment, we extended the work of Gribble and Ostry (1999) and tested whether shoulder muscles compensate for the magnitude of interaction torques arising during self-initiated single-joint elbow movements performed across a range of speeds from different initial elbow orientations. In our second experiment, we tested whether elbow and shoulder muscles compensate for interaction torques introduced by self-initiated single-joint wrist movements. In our third and fourth experiments, we used the same paradigm to test whether feedforward (i.e., self-initiated) and rapid feedback (i.e., reflexive) control of shoulder muscles compensate for interaction torques introduced by changing the orientation of the hand. Taken together, our results demonstrate that the nervous system robustly accounts for intersegmental dynamics across the shoulder, elbow, and wrist, both during self-initiated planar reaching and during responses to unexpected mechanical perturbations.

MATERIALS AND METHODS

Participants. A total of 60 participants (age 18–38 yr; 32 men, 28 women) with no known musculoskeletal or neurological diseases participated in the studies described. Each participant was tested in one of the four experiments. All participants had normal or corrected-to-normal vision and self-reported that they were right hand dominant. The Office of Research Ethics at Western University approved all experimental procedures according to the Declaration of Helsinki, and all participants gave informed written consent before participating in an experiment.

Apparatus. Experiments were performed with a three-degree-of-freedom exoskeleton robot (Interactive Motion Technologies, Boston,

MA) that allows flexion/extension rotations of the shoulder, elbow, and wrist joints in a horizontal plane intersecting the shoulder joint (for details, see Weiler et al. 2015, 2016). Note that although the mass of the exoskeleton influences the overall muscle activity required to move the arm, the inertial properties of the exoskeleton are roughly coaligned with the inertial properties of the arm and are the same for all experimental conditions. The exoskeleton measures movement kinematics of the shoulder, elbow, and wrist joints and can apply torques that flex or extend each independent joint. Visual stimuli were projected downward from a 46-in. LCD monitor (60 Hz, 1,920 × 1,080 pixels; model DX-46L262A12; Dynex, Richfield, MN) onto a semisilvered mirror. The mirror was mounted parallel to the plane of motion and blocked direct vision of the participant's arm. Visual feedback about the participant's hand position was provided between trials by displaying a cursor (purple circle, 1-cm diameter) at the location of the exoskeleton handle on the visual display. Each segment length of the robot was adjusted to fit the participant's arm, so the cursor was aligned with their actual hand position. The lights in the experimental room were extinguished for the duration of data collection.

Experiment 1: Compensating for interaction torques during single-joint elbow movements. Fifteen participants performed 30° of elbow flexion and extension movements, starting from three different initial elbow orientations and at two movement speeds. Each trial began with the participant grasping the exoskeleton handle and moving the projected cursor to a blue circle (i.e., home target; 2-cm diameter) that corresponded to the hand position when the shoulder and elbow joints were at a specific orientation for each condition. We displayed the home target so that the shoulder joint was always positioned at 60° (external angle), and the initial orientation of the elbow could be positioned at either 45°, 60°, or 75° (external angles) for elbow flexion movements and 75°, 90°, or 105° angles for elbow extension movements (Fig. 1, *top left*). The wrist joint was physically locked at 16° in all conditions, including flexion and extension movements. Once participants achieved and remained at one of these joint orientations for 3 s, an instruction about movement speed ("fast" or "slow") was displayed 2 cm above the home target. At the same time, the hand feedback cursor was extinguished and remained off for the rest of the trial. After a short delay (0–1 s, uniform distribution), a white goal
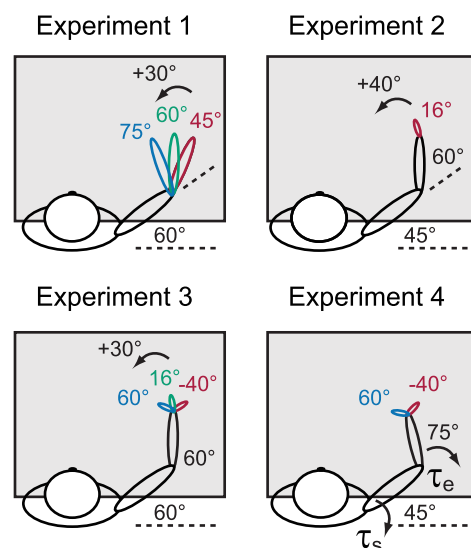

Fig. 1. Experimental setup. Participants were seated and placed their right arm in a three-joint (shoulder, elbow, wrist) robotic exoskeleton that allowed them to perform reaching movements in the horizontal plane. A semisilvered mirror occluded vision of their hand. For clarity, only flexion movement conditions for each experiment are shown, as depicted by the arrows in *experiments 1–3*. Arrows in *experiment 4* represent the multijoint step-torques applied to the shoulder and elbow joints.

target was drawn such that it could be reached with pure elbow flexion or extension (30°). The participant's task was to move the hand into the goal target at the instructed speed. The goal target turned green when movement time, calculated as the time from exiting the start position to entering the goal position, was less than 120 and 220 ms for fast and slow movements, respectively. If movement speed exceeded 220 ms, the goal target turned red. The order of all elbow orientations and movement speeds were randomized. Participants completed a total of 480 trials (2 speeds × 2 directions × 3 initial elbow configurations × 40 repeats per condition). About 2.5 h were required to complete *experiment 1*.

Experiment 2: Compensating for interaction torques during single-joint wrist movements. Fifteen participants performed 40° wrist flexion and extension movements. In this experiment, participants placed their hand into a custom-made hand trough attached to the exoskeleton handle, which kept their fingers straight. Each trial began with the participant moving their hand to a blue circle (i.e., home target; 2-cm diameter) that corresponded to the tip of their index finger when the shoulder, elbow, and wrist joints were at 45°, 60°, and 16° angles, respectively (Fig. 1). Once participants held this posture for 3 s, the cursor indicating the position of the tip of the index finger was extinguished and a white goal target was drawn after a short random delay (0–1 s, uniform distribution) such that it could be reached with 40° of wrist flexion alone (Fig. 1, *top right*). We instructed participants to move the cursor from the home target into the goal target. The goal target turned green when the movement between these targets was less than 150 ms and turned red otherwise. Feedback of the index fingertip position remained off during the movement and reappeared to indicate the start of a new trial. The previous goal target then became the new starting location for a wrist extension movement, and the same sequence of events took place. Participants completed a total of 120 trials (60 wrist flexion and 60 wrist extension). About 1 h was required to complete *experiment 2*.

Experiment 3: Compensating for interaction torques introduced by hand orientation. Fifteen participants performed 30° elbow flexion and extension movements with different hand configurations. Participants used the custom-made hand trough as in *experiment 2*. Participants moved their hand to a blue circle (i.e., home target; 2-cm diameter) that corresponded to the tip of their index finger when the shoulder and elbow were at 60° and the wrist was at a −30°, 16°, or 50° configuration (Fig. 1, *bottom left*). Once participants achieved and remained at one of these joint configurations for 3 s, feedback of index fingertip position was extinguished and a white goal target was then drawn such that it could be reached with elbow rotation alone. The participant's task was to move the hand between the targets within 150 ms while keeping the hand at the specified configuration. The goal target turned green when movement time was within the required time and turned red when it was slower. The order of all wrist configurations was randomized. Participants completed a total of 360 trials (2 directions × 3 wrist configurations × 60 repeats per condition). About 2.5 h were required to complete *experiment 3*.

Experiment 4: Rapid feedback responses at the shoulder account for interaction torques caused by hand orientation. Fifteen participants were instructed to respond to multijoint mechanical perturbations that led to similar shoulder and elbow motion profiles (see Kurtzer et al. 2008) while their hand was positioned in one of two initial orientations. All participants used the hand trough as in *experiments 2* and *3*. At the beginning of a trial, participants moved the tip of the index finger (indicated by a cursor) to a blue circle (i.e., start target; 4-cm diameter) whose center was located above the center of rotation of the participant's wrist when the shoulder and elbow were at 70° and 90°, respectively. After the start target was entered, the exoskeleton gradually applied (over 2 s) a background torque of −2 N·m to the elbow and locked the wrist into two distinct configurations (−40° and 60°). A blue circle was then displayed (i.e., home target; 2-cm diameter) centered at the tip of the participant's index finger when the shoulder and elbow were at 45° and 75°, respectively.

Participants were instructed to move the cursor to the home target while counteracting the background load at the elbow.

After the cursor was maintained in the home target for a randomized duration (1.0–2.5 s, uniform distribution), the cursor was removed and a step-torque (i.e., perturbation) was applied to the shoulder and elbow joints, which rapidly displaced the participant's hand outside the home target. Critically, we applied a specific combination of torques at the shoulder and elbow so that this perturbation would lead to similar motion profiles at the shoulder and elbow joints in the two wrist configurations (Fig. 1, *bottom right*). The torques that generated these motion profiles (minimal shoulder motion and substantial elbow motion) were −0.5 and −5.5 N·m torques at the shoulder and elbow when the wrist was locked at −40° and −0.3 and −5.5 N·m torques at the shoulder and elbow when the wrist was locked at −60°, respectively (i.e., *load combination 1*). We also coupled each of these torques with the other wrist configuration (i.e., *load combination 2*). Note that trials from *load combination 2* were only present to ensure the perturbation was unpredictable and were not analyzed in detail. After perturbation onset, participants were instructed to quickly bring the cursor back into a goal target (4-cm diameter centered on the home target). If the participant moved the cursor into the goal target within 375 ms of perturbation onset, the target circle changed from white to green; otherwise, the target circle changed from white to red. Regardless of trial outcome, all torques were gradually removed 1,300 ms after perturbation onset. The order of all wrist configurations and perturbations was randomized. Participants completed a total of 300 trials (2 torques × 2 wrist configurations × 75 repeats per condition). About 2.5 h were required to complete *experiment 4*.

Common experimental features. Before data collection began for all experiments, participants performed normalization trials. In these trials, participants were instructed to move the cursor to a blue circle (i.e., home target; 2-cm diameter) that was centered at the robot's handle (*experiment 1*) or the tip of the participant's index finger (*experiments 2–4*) when the shoulder, elbow and wrist joints were at 45°, 60°, and 16°, respectively. Once the cursor was in the home target, the exoskeleton gradually applied torques to either the shoulder, elbow, or wrist joints, which plateaued at a constant torque of ±2 N·m. Participants were instructed to counter these torques while maintaining the cursor in the home target for 4 s. After this period, the joint torques were turned off. The order of the normalization trials, which included flexion and extension at each of the three joints, was randomized. Participants completed four trials of each condition.

For all experiments, rest breaks were given throughout or when requested. Before data collection began, participants completed practice trials until they comfortably achieved ~70% success rates (~10 min).

Muscle activity. In all experiments we collected muscle activity using surface EMG electrodes (Delsys Bagnoli-8 system with DE-2.1 sensors; Boston, MA). The participants' skin was abraded with rubbing alcohol, and contacts were coated with conductive gel. Electrodes were then placed on the skin surface overlying the belly of six muscles for *experiments 1–3* ([pectoralis major clavicular head (PEC), shoulder flexor; posterior deltoid (PD), shoulder extensor; biceps brachii long head (BB), shoulder and elbow flexor, wrist supinator; triceps brachii lateral head (TR); elbow extensor; flexor carpi ulnaris (WF), wrist flexor; extensor carpi radialis (WE), wrist extensor]. Electrodes were oriented parallel to the orientation of muscle fibers. All but wrist muscles were also recorded in *experiment 4*. A reference electrode was placed on the participant's left clavicle. EMG signals were amplified (gain = 10^3), bandpass filtered (20–450 Hz), and then digitally sampled at 2,000 Hz. Normalization trials (see above) before each experiment were used to normalize muscle activity such that a value of 1 represents a given muscle sample's mean activity during movements to counter a 2 N·m torque (see Pruszynski et al. 2008).

Data analysis. All joint kinematics (i.e., hand position and joint angles) were sampled at 500 Hz and then low-pass filtered (12 Hz, 2-pass, 4th-order Butterworth). EMG data were bandpass filtered (20–500 Hz, 2-pass, 2nd-order Butterworth) and full-wave rectified. For scoring the onset of phasic EMG bursts, the rectified signals were low-pass filtered (50 Hz, 2-pass, 12th-order Butterworth). For *experiments 1–3*, all data were aligned on movement onset. Movement onset was defined as 5% of peak angular velocity of the elbow joint for *experiments 1* and *3*, and 5% of peak angular velocity of the wrist joint for *experiment 2*. All data were aligned on perturbation onset for *experiment 4*.

In *experiments 1–3*, we assessed whether muscles at stationary joints compensate for interaction torques as a function of limb configuration and speed. For these experiments, we calculated the torques at the relevant stationary joint (Fig. 2) by simulating three joint planar reaching with the joint configurations and timing requirements of each experiment along with previously published anthropometric values (Winter 2009). To compare the amplitude of muscle activity across these different conditions, we calculated the mean amplitude of phasic muscle activity across a fixed time window (see Debicki and Gribble 2005). We used a fixed time window from −200 to +100 ms relative to movement onset in *experiments 1* and *3*, and from −100 to +100 ms relative to movement onset in *experiment 2*. These windows were chosen to capture the agonist burst of EMG activity in each of the experiments, and our results did not qualitatively change with small changes in the start and end of the analysis window.

We assessed the timing of muscle activity by calculating the onset of the first phasic EMG burst of each muscle in each trial. For each trial we computed baseline EMG activity over a fixed 100-ms window, 400 ms before the start of movement. The onset of the first EMG burst was scored as the time at which the EMG signal rose 3 SD above the mean baseline level and remained above that level for 50 ms. A research assistant, unaware of the study hypotheses, performed additional manual inspection of the results of this algorithm and confirmed, rejected (10%), or re-marked these onsets values relative to movement onset.

In *experiment 4* we investigated whether shoulder muscles compensated for limb dynamics related to hand orientation when countering mechanical perturbations. To test whether the short- and long-latency stretch response of a shoulder flexor muscle accounts for hand orientations, we binned PEC EMG into previously defined epochs of

time (Pruszynski et al. 2008). This included a pre-perturbation epoch (PRE; −50 to 0 ms relative to perturbation onset), the short-latency stretch response (R1; 20–50 ms), the long-latency stretch response (R2/3; 50–100 ms), and the so-called voluntary response (VOL; 100–150 ms).

Data processing was performed using MATLAB (The Math-Works, Natick, MA), and statistical analyses were performed using R (RStudio, Boston, MA). We performed different statistical tests (e.g., repeated-measures ANOVA with Tukey's test for multiple comparisons, paired and single-sample *t*-tests with Holm-Bonferroni correction for multiple *t*-tests) as appropriate for each of the four experiments. Details of these procedures are provided in RESULTS. Experimental results were considered statistically significant if the corrected *P* value was <0.05.

RESULTS

Experiment 1: Compensating for interaction torques during single-joint elbow movements. We instructed participants to move the tip of their index finger between two targets. The start and end targets were always positioned so that flexing or extending only the elbow joint would successfully transport the hand between the two targets (Fig. 1). We manipulated the start and end target location, as well as the required movement speed, to test whether shoulder muscle activity compensates for variations in the amplitude of interaction torques that arise as a function of the elbow's initial configuration and the speed of rotation (Fig. 2). Participants quickly learned the task and had little difficulty reaching the goal target within the imposed speed and accuracy constraints (mean success rate = 90%). We included all trials in the analysis. Although we did not explicitly enforce a particular trajectory between the two targets, participants achieved the required movement by rotating their elbow joint while keeping the shoulder and wrist joints relatively fixed (Fig. 3, *A* and *B*).

We used two-way repeated-measures ANOVAs (one for elbow flexion and one for elbow extension) to test whether the peak velocity of elbow rotation differed between our three elbow orientation and two speed conditions. For both elbow flexion (Fig. 3*C*) and extension movements (Fig. 3*D*), we found a reliable effect of speed condition on peak elbow rotation velocity (flexion: $F_{1,78} = 23.7$, $P < 0.0001$; extension: $F_{1,78} = 25.6$, $P < 0.0001$), but no significant effect of elbow orientation ($F_{2,78} = 0.006$, $P = 0.99$; $F_{2,78} = 1.134$, $P = 0.32$) or interaction ($F_{2,78} = 0.053$, $P = 0.94$; $F_{2,78} = 0.044$, $P = 0.95$). On average, fast movements were 36% faster than slow movements for both flexion and extension directions.

Figure 4 shows the group-average shoulder flexor (PEC; *A* and *B*) and extensor (PD; *D* and *E*) muscle activity associated with fast (*left*) and slow (*right*) movements at each initial elbow configuration. Despite minimal shoulder rotation, we found substantial shoulder muscle activity before movement onset. We found no evidence of substantial co-contraction at the shoulder; rather, agonist shoulder muscle activation appeared at the muscle appropriate for counteracting the interaction torques that were about to arise due to the upcoming forearm rotation (i.e., shoulder flexors for elbow flexion and shoulder extensors for elbow extension). We quantified the magnitude of agonist shoulder muscle activity in each condition by computing the mean muscle activity over a fixed time window (−200 to 100 ms) relative to movement onset (see METHODS). For each participant, we related the agonist muscle
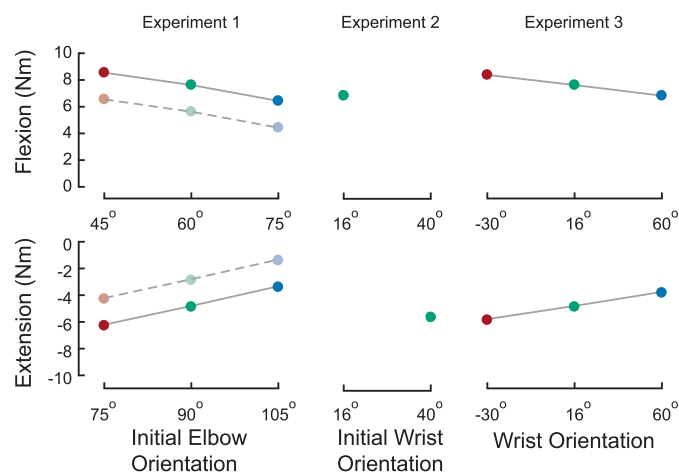

Fig. 2. Calculated interaction torques from a simulation of three-joint planar reaching. Peak torque at the shoulder (*experiments 1* and *3*) and elbow joints (*experiment 2*) during single-joint elbow and wrist movements, respectively. *Top* and *bottom* rows indicate flexion and extension movements, respectively. For *experiment 1*, fast and slow movements are represented as solid and dashed lines, respectively. Simulated joint configurations and movement timing are from our experiments (see METHODS). Anthropomorphic data are from Winter (2009).
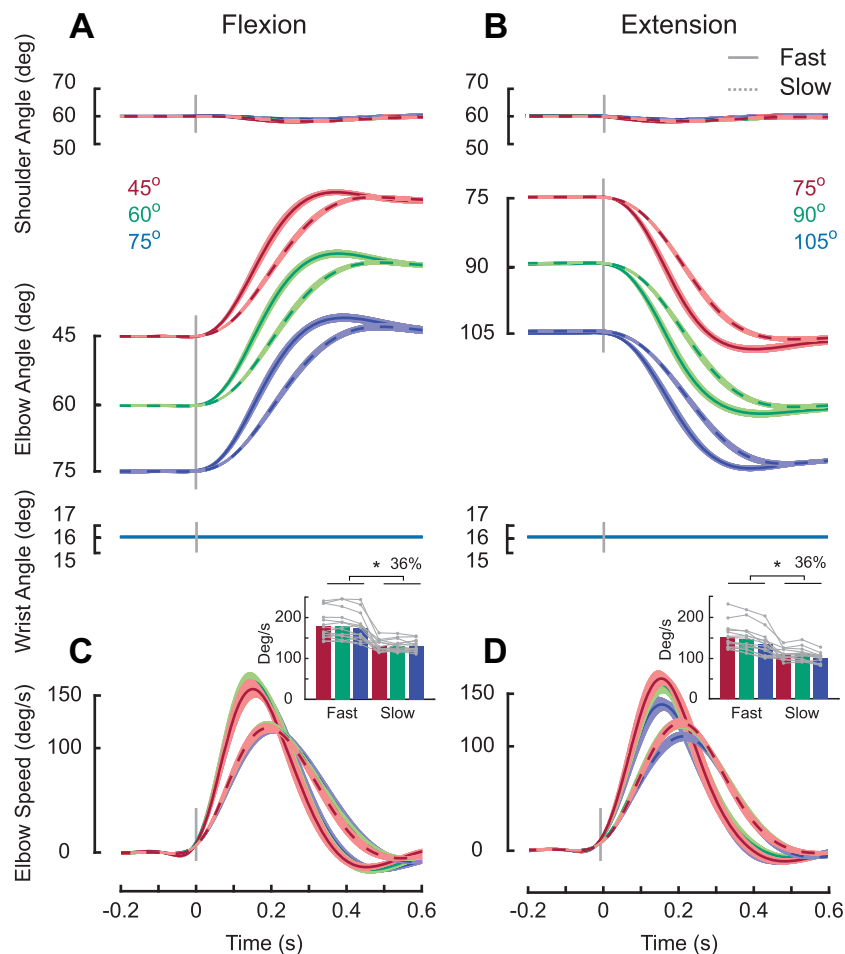
Fig. 3. Reaching behavior in *experiment 1*. *A*: kinematics of single-joint elbow movements are shown for 3 different elbow configurations and 2 movement speeds. Thick lines represent the group mean of the kinematics of the shoulder, elbow, and wrist joints during elbow flexion. Fast and slow movements are represented as solid and dashed lines, respectively. Shaded areas represent SE. Data are aligned on movement onset. *B*: kinematics of extension movements are shown using the same format as *A*. *C*: elbow velocity is shown. The *inset* summarizes peak velocity as a function of elbow configuration and instructed movement speed. Bars represent the mean peak velocity across participants, and each gray line represents the mean peak velocity of a single participant. *$P < 0.05$ indicates a reliable effect of speed (see text). *D*: extension movements are shown using the same format as *C*.

activity to the three initial joint configurations using linear regression (Fig. 4, *C* and *F*). We predicted a negative relationship between muscle activity and initial external angle because, under our experimental constraints, increasing the external angle decreases the interaction torques at the shoulder (Gribble and Ostry 1999; see also Fig. 2). Consistent with our prediction, a one-sample *t*-test of each individual's slope revealed a reliable negative relationship for both fast and slow elbow flexion (fast: $t_{14} = -6.5$, $P < 0.0001$; slow: $t_{14} = -4.361$, $P = 0.0006$) and extension movements ($t_{14} = -2.39$, $P = 0.03$; $t_{14} = -3.36$, $P = 0.004$). We also predicted larger shoulder muscle activity for the faster movement speed because interaction torques at the shoulder scale with elbow rotation velocity and acceleration (Fig. 2). A one-sample *t*-test of each individual's intercept confirmed our prediction in flexion and extension movements (flexion: $t_{14} = 5.82$, $P < 0.0001$; extension: $t_{14} = 5.64$, $P < 0.0001$).

Figure 5 shows a histogram of all shoulder and elbow muscle onset times for all subjects relative to movement onset for elbow flexion (*A* and *B*) and extension (*D* and *E*) trials. These histograms indicate that shoulder muscle activity almost always begins well before movement onset (i.e., elbow rotation). For elbow flexion and extension trials, PEC and PD muscle activity reliably preceded movement onset by 160 (6) ms [mean (SE); $t_{14} = -26.5$, $P < 0.0001$; one-sample *t*-test vs. 0) and 150 (4) ms ($t_{14} = -38.1$, $P < 0.0001$), respectively. To examine differences in onset times between shoulder and

elbow muscles, we superimposed the cumulative distribution function of shoulder and elbow muscle onset times relative to movement onset in Fig. 5, *C* and *F*. Statistical analysis revealed that PEC onsets reliably preceded BB onsets by a modest 10 (4) ms ($t_{14} = -2.4$, $P = 0.02$) for flexion trials. On the other hand, we found no statistically reliable difference between onset times in PD and TB muscles for extension trials ($t_{14} = -1.6$, $P = 0.14$), although the data showed a similar trend (mean difference 6 ms).

Last, we examined the correlation between shoulder and elbow muscles in terms of their amplitude of activation (Fig. 6, *A* and *B*) and onset time (Fig. 6, *C* and *D*) across movements. We predicted a positive relationship between shoulder and elbow muscle activity magnitude and onset timing, consistent with a process that actively compensates for intersegmental dynamics on a trial-by-trial basis. As predicted, in terms of magnitude, all 15 participants showed a significant positive correlation for flexion movements, and 14 participants showed a significant positive correlation for extension movements. Similarly, in terms of timing, 14 of 15 participants showed a significant positive correlation for both flexion and extension movements (note that fast and slow movements were combined).

Experiment 2: Compensating for interaction torques during single-joint wrist movements. We investigated whether elbow muscles account for interaction torques introduced by wrist movements (Fig. 2). The start and end targets were always
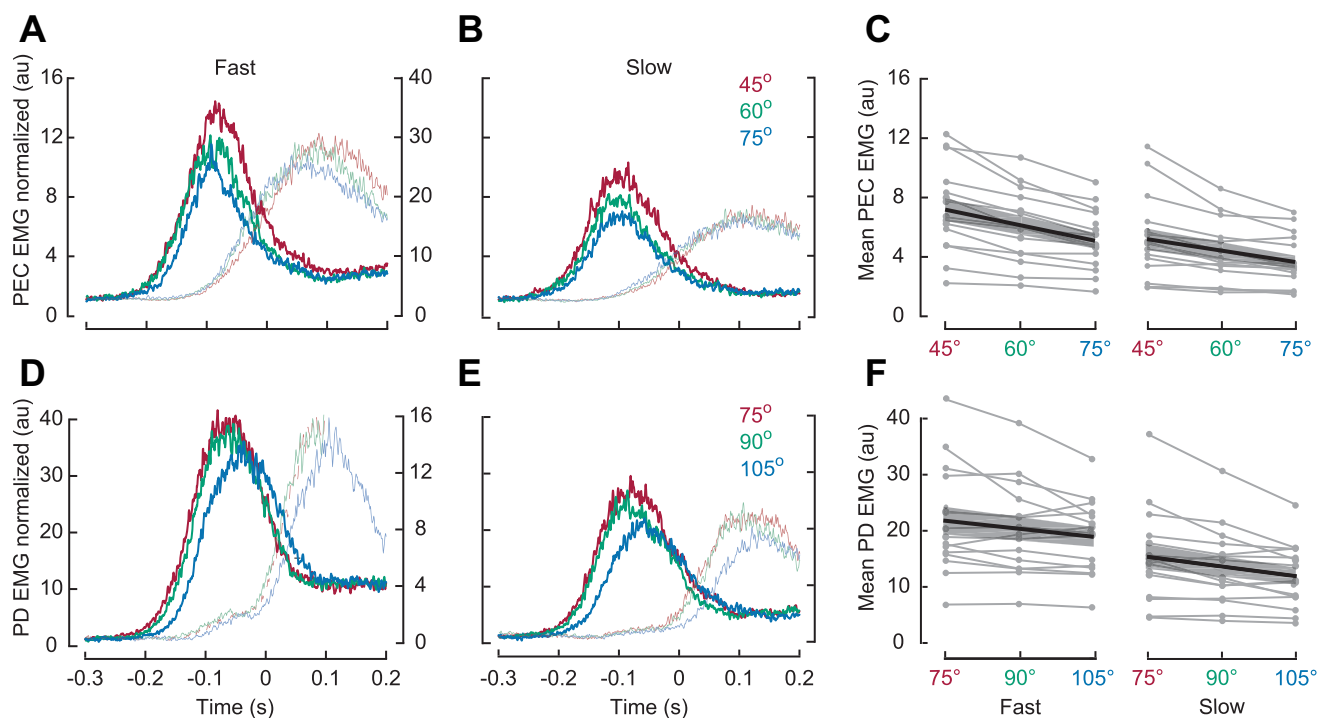
Fig. 4. Muscle activity in *experiment 1*. *A*: thick and thin lines represent average agonist (PEC) and antagonist (PD) muscle activity during fast flexion movements. Initial configuration is depicted by line color. EMG data are normalized as described in METHODS. Data are aligned on movement onset. *B*: EMG data are shown using the same format as *A* for movements in the slow condition. *C*: individual data (gray lines) and mean regression slopes (black line; shaded area represents SE) between mean agonist muscle activity and elbow orientations during elbow flexion movements at different speeds. Mean agonist muscle is shown in a fixed time window (-200 to 100 ms relative to movement onset). *D–F*: data for elbow extension movements are shown using the same format as *A–C* for agonist (PD) and antagonist (PEC) muscle activity. au, Arbitrary units.

placed along an arc centered on the wrist joint so that flexing or extending only the wrist joint would successfully transport the hand between the targets (Fig. 1). Participants quickly learned the task and had little difficulty reaching the goal target within the imposed speed and accuracy constraints (mean success rate = 99%). Figure 7 shows the average kinematics of the elbow and wrist joints during single-joint wrist flexion and extension movements, respectively. Similar to *experiment 1*, although we did not give explicit instructions about how the participants should complete the required movement, participants did so by almost exclusively rotating the wrist joint.

Figure 8 shows average muscle activity for wrist flexion (*A* and *B*) and wrist extension movements (*D* and *E*). These plots indicate that elbow muscle activity preceded movement onset and that these were directional responses appropriate for counteracting the interaction torques about to arise due to upcoming hand rotation. We quantified this compensation by computing the mean muscle activity in a fixed time window (-100 to 100 ms) relative to movement onset. For wrist flexion movements (Fig. 8*C*), a one-sample *t*-test showed that both the WF ($t_{14} = 6.3$, $P < 0.0001$, 374% increase) and BB ($t_{14} = 3.2$, $P = 0.006$, 58% increase) muscles significantly increased their activity relative to baseline. For wrist extension movements (Fig. 8*F*), a one-sample *t*-test showed that both the WE ($t_{14} = 5.3$, $P = 0.0001$, 280% increase) and TB ($t_{14} = 3.5$, $P = 0.003$, 72% increase) muscles significantly increased their activity relative to baseline.

As evident from the average muscle responses in Fig. 8, we found that both BB ($t_{14} = -33.7$, $P < 0.0001$) and WF

($t_{14} = -26.2$, $P < 0.0001$) muscle activity significantly preceded wrist flexion movement onset by 100 (3) and 90 (3) ms, respectively (Fig. 9*A*). Similarly, we found that TB ($t_{14} = -21.8$, $P < 0.0001$) and WE ($t_{14} = -16.3$, $P < 0.0001$) muscle activity significantly preceded wrist extension movement onset by 100 (4) and 70 (4) ms, respectively (Fig. 9*C*). We further investigated whether there was a difference in onset times between muscles by using paired *t*-tests (one for wrist flexion and one for wrist extension movements) applied to average onset times. We found a reliable difference in onset times for both wrist flexion and extension movements (flexion: $t_{14} = -2.3$, $P = 0.003$; extension: $t_{14} = -5.9$, $P < 0.0001$) whereby elbow muscle activity preceded the wrist muscle activity (Fig. 9, *B* and *D*).

Last, we examined the correlation between elbow and wrist muscle activity on a trial-by-trial basis. As in *experiment 1*, we expected a positive relationship between elbow and wrist muscle activity in terms of both amplitude and onset timing. A one-sample Wilcoxon rank-sum test on individual correlation coefficients revealed a reliable positive relationship between elbow and wrist muscle activity magnitude for wrist flexion trials ($W_{14} = 116$, $P < 0.0004$; 9 participants showed individually significant positive correlations) but not for wrist extension movements ($W_{14} = 77$, $P = 0.35$; 5 participants). We also found reliable positive relationships between elbow and wrist onset timings for both wrist flexion and extension movements (flexion: $W_{14} = 120$, $P < 0.0001$; extension: $W_{14} = 120$, $P < 0.0001$; for both flexion and extension, all participants showed significant positive correlations).
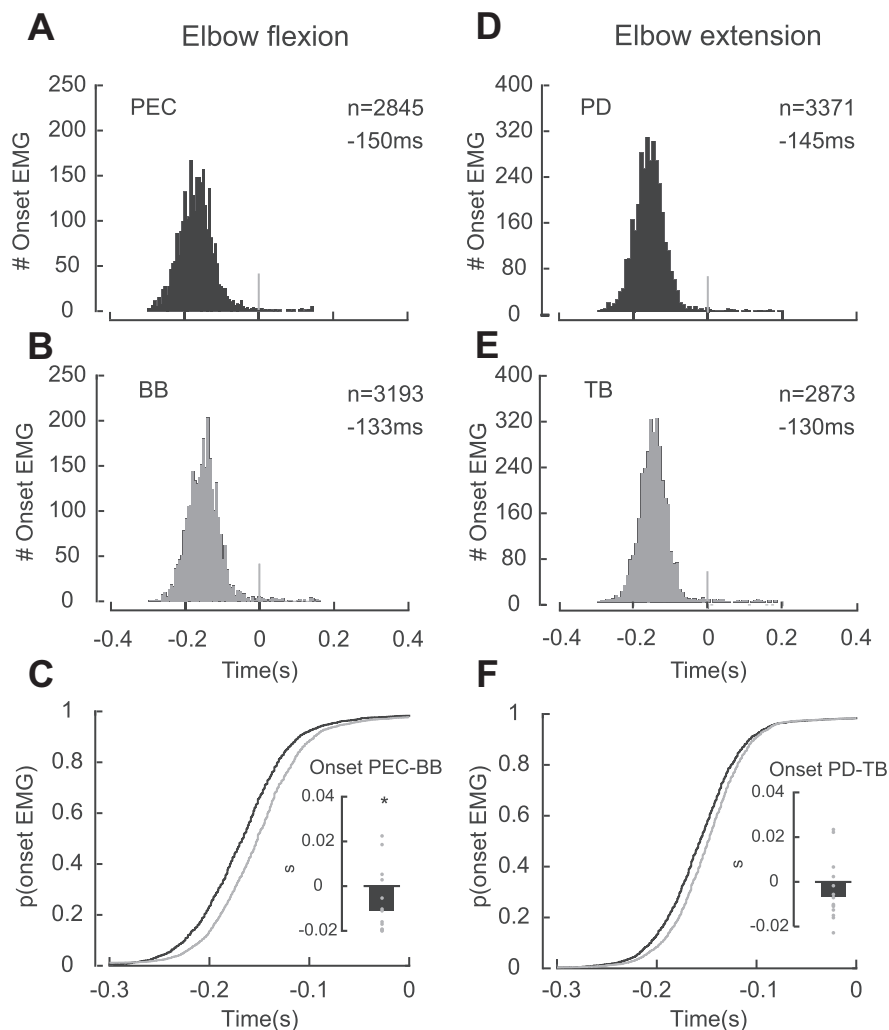
Fig. 5. Muscle onset timing in *experiment 1*. Histograms show onset times of PEC (*A*) and BB (*B*) muscles during elbow flexion movements. Data are aligned on movement onset. *C*: cumulative distributions of onset times of shoulder and elbow muscles are shown for elbow flexion movements. The *inset* shows the difference between mean shoulder and elbow onset times. *$*P < 0.05$, reliable effect (see text). *D–F*: data for elbow extension movements are shown using the same format as *A–C* for onset times of PD and TB muscles.

Experiment 3: Compensating for interaction torques introduced by hand orientation. We assessed whether shoulder muscle activity compensates for differences in the interaction torques introduced by changing hand orientation during single-joint elbow movements (Fig. 2). That is, participants made the same elbow movement as in *experiment 1* with their wrist beginning in three different configurations, and we tested whether shoulder muscle activation accounted for how hand orientation influenced interaction torques at the shoulder caused by forearm rotation. As expected, participants completed the task mostly via single-joint rotations at the elbow joint (Fig. 10), and they had little difficulty reaching the goal target within the imposed speed and accuracy constraints (mean success rate = 95%).

Figure 11 illustrates the average agonist muscle activity at the PEC and PD muscles during elbow flexion (*A*) and extension (*C*), respectively. Qualitatively, shoulder muscle activity scaled for the three different initial wrist configurations, and this scaling was consistent with the magnitude of interaction torques introduced by changing hand orientation. We quantified this relationship by calculating the magnitude of shoulder muscle activity in each hand orientation condition in a fixed time window (−200 to 100 ms) relative to movement onset. We performed linear regression for each muscle sample to determine whether there was a reliable relationship between

shoulder muscle activity and the initial wrist configurations. A one-sample *t*-test of the individual slopes revealed a reliable negative slope for PEC muscle activity during elbow flexion ($t_{14} = -5.9$, $P < 0.0001$; Fig. 11*B*) and for PD muscle activity during elbow extension ($t_{14} = -5.0$, $P = 0.0001$; Fig. 11*D*).

Figure 12, *A* and *B*, shows the cumulative distribution of onset times of the relevant shoulder, elbow, and wrist muscles for elbow flexion and extension movements, respectively. We investigated differences in onset times across muscles and, in this case, hand orientation with a two-way repeated-measures ANOVAs (one for elbow flexion and one for elbow extension). For elbow flexion movements, we found a reliable effect of muscle ($F_{2,117} = 5.4$, $P = 0.005$), but not the effect of orientation ($F_{2,117} = 0.25$, $P = 0.78$), and no interaction ($F_{4,117} = 0.055$, $P = 0.99$). Tukey post hoc tests showed that PEC muscle activity reliably preceded BB muscle activity ($P = 0.001$) by 20 ms ($P = 0.0011$) and that BB muscle activity preceded WF muscle activity by 7 ms ($P = 0.0016$). For elbow extension movements, we found a reliable effect of orientation ($F_{2,117} = 4.0$, $P = 0.02$) as well as muscle ($F_{2,117} = 5.2$, $P = 0.006$), but no interaction ($F_{4,117} = 0.96$, $P = 0.42$). Tukey post hoc tests showed that muscle onset times in the −40° hand orientation preceded those in the 16° hand orientation by 25 ms ($P = 0.0026$), and the 60° hand orientation by 24 ms ($P = 0.0053$). In addition, Tukey post hoc
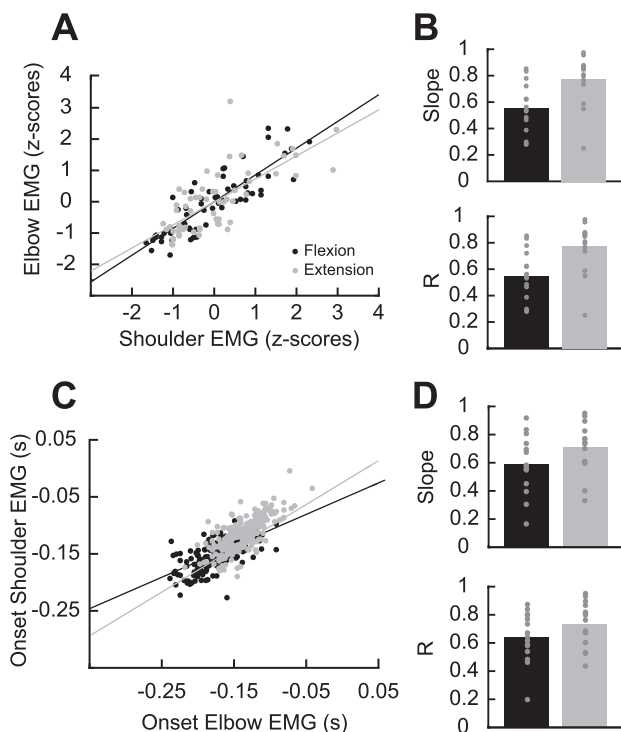
Fig. 6. Trial-by-trial relationships between muscles in *experiment 1*. *A*: exemplar correlation between muscle activity at the shoulder and elbow. Each dot represents mean muscle activity in a predefined epoch from a single trial (−200 to 100 ms relative to movement onset). Values are *z*-normalized. *B*: group mean slopes and correlation coefficients (*R*). Each dot represents data from a single participant. *C* and *D*: data for correlation between muscle onset times are shown using the same format as *A* and *B*, respectively.

tests showed that TB muscle activity preceded PD muscle activity by 9 ms ($P = 0.0007$) and that TB muscle activity preceded the WE muscle activity by 22 ms ($P = 0.005$).

Experiment 4: Rapid feedback responses at the shoulder account for interaction torques caused by hand orientation. Our last experiment mimicked *experiment 3* but examined feedback control. That is, we tested whether rapid feedback responses to mechanical perturbations compensate for interaction torques arising due to the orientation of the hand. We did so by extending our previously established paradigm (Kurtzer et al. 2008) to the three-joint situation. Briefly, for two wrist configurations, we applied shoulder and elbow torques that yielded very similar shoulder and elbow motion (see METHODS). This allowed us to directly test whether rapid feedback responses in shoulder muscles modulated their muscle activity according to the underlying torque at the shoulder, which differs because of the intersegmental effects introduced by the different wrist configurations.

Figure 13 shows the average kinematics for each participant at the shoulder, elbow, and wrist joints with the wrist initially in flexion (60°; *A*) or extension (−40°; *B*). Note the highly similar motion at the shoulder (median difference = 0.003°) and elbow (0.04°) for the two hand orientations, which was achieved by applying higher shoulder torque for the wrist extension condition (see METHODS; Fig. 13, *C* and *D*).

Figure 14*A* presents the average shoulder (PEC) muscle activity for the two initial hand orientations. We focused on the shoulder because the elbow had the same underlying torques for both hand orientations. Qualitatively, we observed no

evoked shoulder activity during the short-latency epoch. This was expected given that the perturbation caused almost no local shoulder motion. In addition, the mean response in the long latency and voluntary epochs showed larger responses for the wrist configuration that involved greater underlying shoulder torque. Statistical analysis confirmed that this was a highly reliable pattern. Paired *t*-tests showed no significant difference in average muscle activity as a function of load condition within the short-latency epoch ($t_{14} = -0.5$, $P = 0.626$, Cohen's $d = 0.128$) but did reveal reliable effects in the long-latency ($t_{14} = -4.1$, $P = 0.001$, $d = 1.05$) and voluntary epochs ($t_{14} = -3.7$, $P = 0.002$, $d = 0.95$) that were appropriate for countering the applied shoulder torques (Fig. 14*B*).

DISCUSSION

Summary. We examined how robustly the nervous system accounts for intersegmental dynamics across the shoulder, elbow, and wrist joints during both feedforward (i.e., self-initiated) and feedback (i.e., reflexive) control. In *experiment 1*, we found that shoulder muscle activation predictively scaled according the magnitude of upcoming interaction torques, as a function of both elbow configuration and movement speed. In *experiment 2*, we found that elbow muscle activation predictively scaled to compensate for interactions torques during single-joint wrist movement. In *experiment 3*, we found that shoulder muscle activity predictively scaled according to the interaction torques introduced by different hand orientations during single-joint elbow movement. In *experiment 4*, we found that feedback responses at the shoulder evoked by a mechanical perturbation that caused single-joint elbow motion also accounted for hand orientation, starting ~50 ms after perturbation onset (i.e., within the long-latency epoch). Taken together, our results demonstrate that the nervous system robustly accounts for intersegmental dynamics across the proximal to distal musculature of the arm, and does so for both feedforward and feedback control.
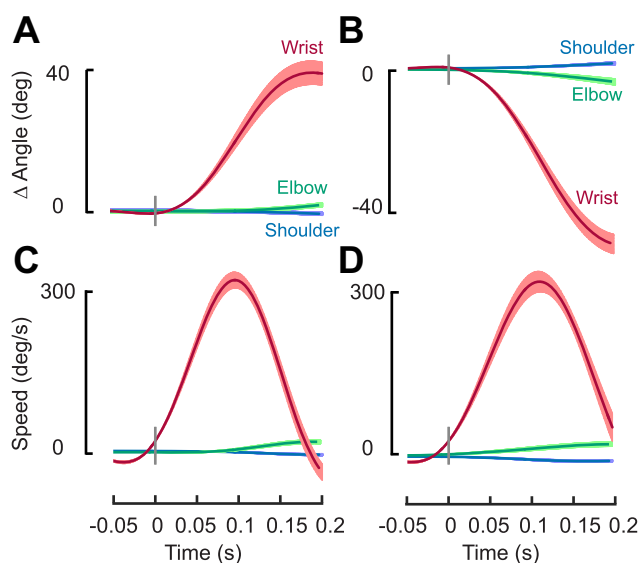

Fig. 7. Reaching behavior in *experiment 2*. *A* and *B*: average kinematic profiles for the shoulder, elbow, and wrist joints for flexion and extension conditions in *experiment 2*, respectively. Data are aligned on movement onset. Shaded areas represent SE. *C* and *D*: data for wrist angular velocity are shown using the same format as *A* and *B*, respectively.
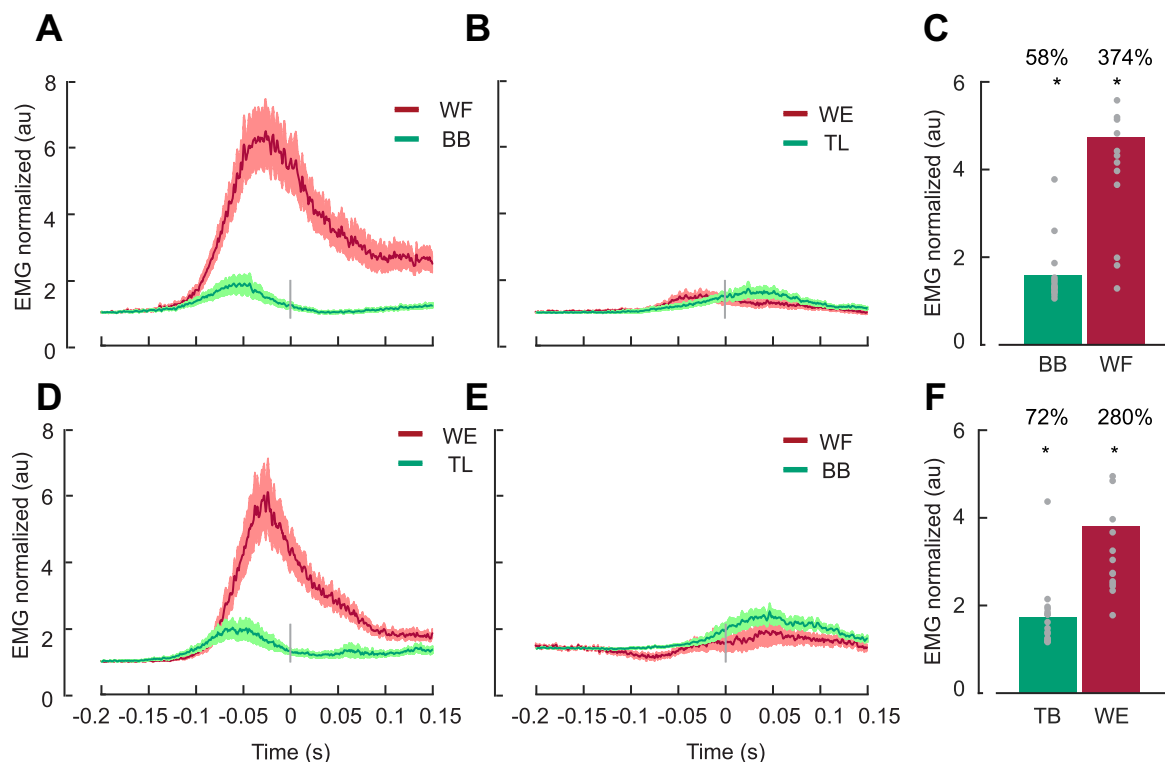
Fig. 8. Muscle activity in *experiment 2*. Graphs show normalized mean muscle activity of BB and WF muscles (*A*) and of their respective antagonist muscles (TB and WE; *B*) during a wrist flexion movement. Data are aligned on movement onset. Shaded areas represent SE. *C*: mean agonist muscle activity (−100 to 100 ms relative to movement onset) is shown. *$*P < 0.05$, reliable effects (see text). *D–F*: data for extension movements are shown using the same format as *A–C*, respectively.

Accounting for interaction torques during feedforward control. Many studies have investigated how the nervous system deals with interaction torques during self-initiated reaching by having participants make single-joint movements when multiple joints are free to move (Almeida et al. 1995;

Fig. 9. Muscle onset timing in *experiment 2*. *A*: mean onset times of BB and WF muscles during flexion movements are shown for *experiment 2*. Gray lines indicate data from individual participants. *$*P < 0.05$, reliable effect (see text). *B*: difference of onset times between BB and WF muscles is shown. Each dot represents data from an individual participant. *C* and *D*: data for wrist extension movements are shown using the same format as *A* and *B*, respectively.

Corcos et al. 1989; Galloway and Koshland 2002; Gottlieb 1998; Gribble and Ostry 1999; Koshland et al. 1991). These studies have established that muscles spanning joints that are adjacent to the moving joint contract before movement onset and, as such, predictively compensate for the interaction torques about to arise because of the movement. Such compensation has been demonstrated for shoulder muscles during pure elbow movements (Almeida et al. 1995; Corcos et al. 1989; Galloway and Koshland 2002; Gribble and Ostry 1999), elbow muscles during pure shoulder movements (Almeida et al. 1995; Galloway and Koshland 2002; Gribble and Ostry 1999), and wrist muscles during pure elbow movements (Koshland et al. 1991). The results of our first two experiments confirm and extend these previous findings by demonstrating that muscle activity at the shoulder joint scales according to the predicted magnitude of the interaction torques during single-joint elbow movement in different elbow configurations and movement speeds (*experiment 1*) and that muscle activity at the elbow joint scales according to interaction torques introduced by single-joint wrist movement (*experiment 2*).

Accounting for intersegmental dynamics becomes more complex in a three-joint scenario because interaction torques arise at all joint segments (for an even more complex scenario involving torso and whole arm movement, see Pigeon et al. 2003). We investigated whether the nervous system accounts for interaction torques across three joints by having participants perform single-joint elbow movements with different wrist configurations (*experiment 3*). Doing so requires different torques to be generated at the shoulder as a function of the hand orientation. An important point to note is that these torque demands are smaller than the torque demands created by the
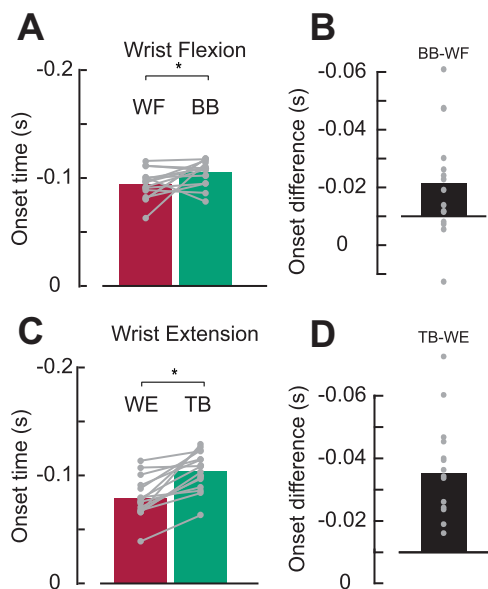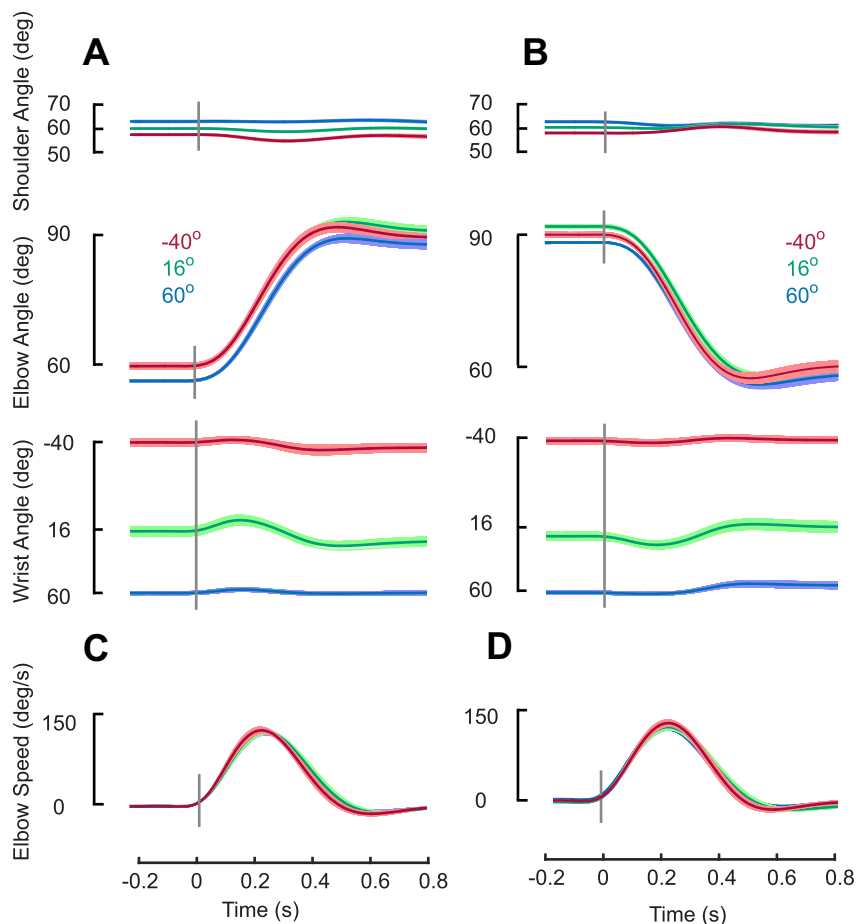
Fig. 10. Reaching behavior in *experiment 3*. Graphs show kinematics of the shoulder, elbow, and wrist joints (*A*) and velocity profiles of the elbow joint (*C*) during flexion movements in *experiment 3*. Data are aligned on movement onset. Shaded areas represent SE. *B* and *D*: data for elbow extension movements are shown using the same formats as *A* and *C*, respectively.

two-joint situations studied in *experiments 1* and *2*. Thus it seemed possible the nervous system would use a qualitatively different control strategy to counter these smaller torque demands. For example, the nervous system could have countered

these interaction torques by co-contracting shoulder agonist and antagonist muscles, thereby increasing the stiffness of the joint and limiting shoulder motion. Indeed, the control of limb stiffness can be an important control scheme in unstable
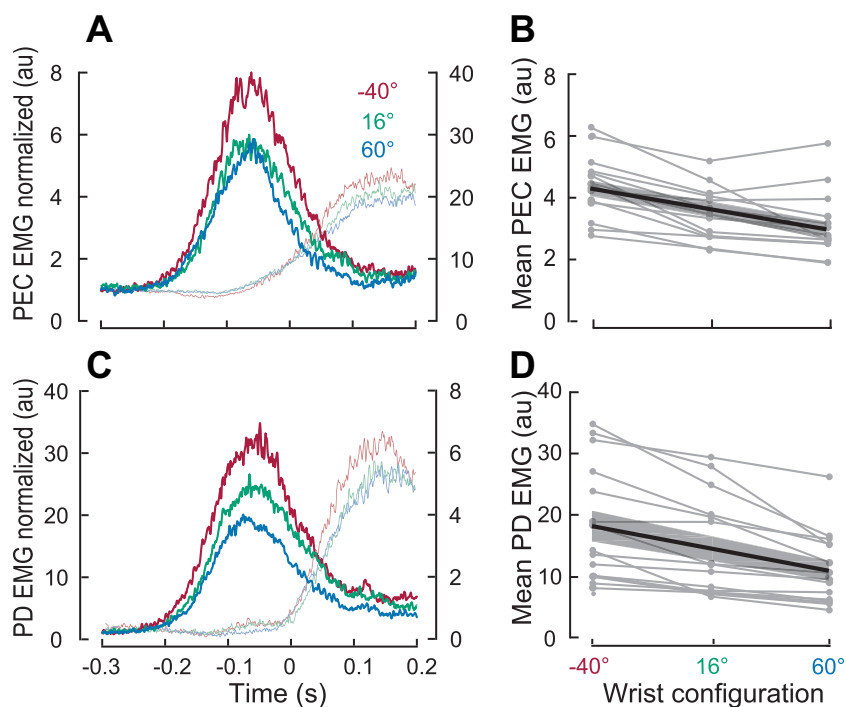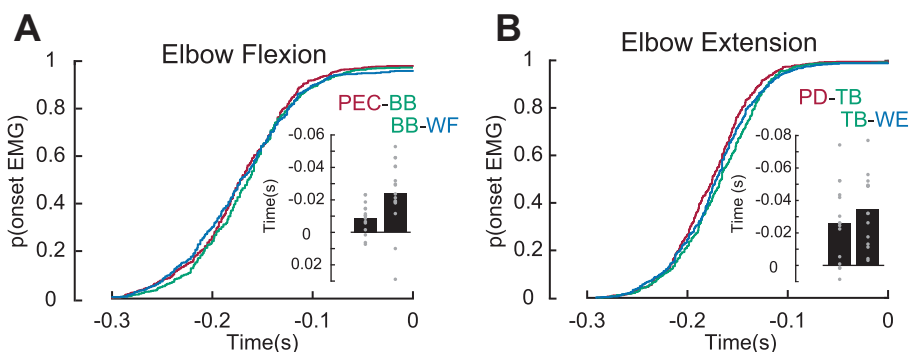

Fig. 11. Muscle activity in *experiment 3*. Shoulder muscles compensate for the magnitude of interaction torques introduced by changing wrist configuration. *A*: average PEC muscle activity is shown during elbow flexion movements in 3 different wrist configurations. Data are aligned on movement onset. *B*: individual data (gray lines) and mean regression slope (black line; shaded area represents SE) between mean agonist muscle activity (−200 to 100 ms relative to movement onset) and the 3 wrist configurations. *C* and *D*: data for elbow extension movements are shown using the same format as *A* and *B*, respectively.

Fig. 12. Muscle onset timing in *experiment 3*. *A*: cumulative distributions of onset times of shoulder, elbow, and wrist muscles during flexion movements are shown for *experiment 3*. Insets represent the group average onset timing difference between muscle pairs. Each gray dot represents the mean onset time difference from a single participant. *B*: data for elbow extension movements are shown using the same format as *A*.

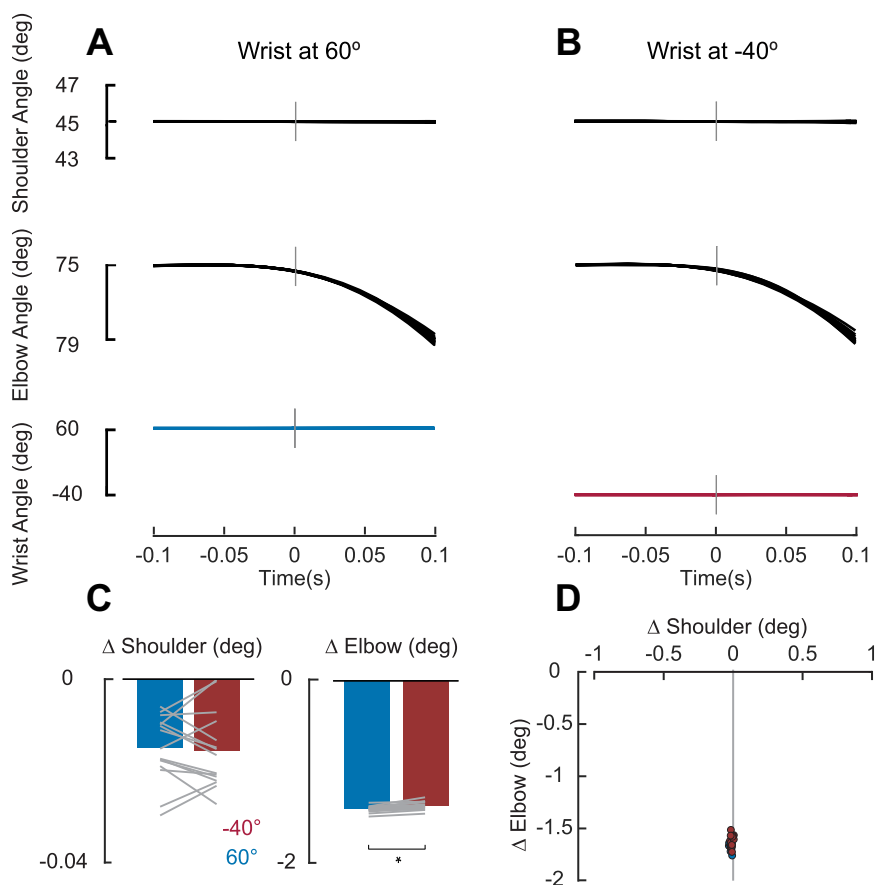**A** Elbow Flexion — **B** Elbow Extension

environments (Burdet et al. 2001; Franklin et al. 2007; Hogan 1985; McIntyre et al. 1996; Milner 2004). However, we found little evidence of co-contraction. Rather, we observed marked phasic activity of shoulder agonist muscles that predicted the magnitude of interaction torques introduced by wrist configuration (Fig. 11). These findings suggest that accounting for intersegmental dynamics is a core computation for the feedforward control of reaching movements that is evident for even very small changes in speed and limb configuration across multiple joints.

Predicting interaction torques during feedforward control. Previous findings have emphasized that during single-joint movement, muscles at the stationary joint are activated before movement onset, indicating that the nervous system compensates for interaction torques in a predictive manner (Almeida et al. 1995; Gribble and Ostry 1999; Koshland et al. 1991; Sainburg et al. 1995, 1999). Our findings are consistent with

this type of organization (Figs. 5, 9, and 12). More interestingly, Gribble and Ostry (1999) demonstrated a particular temporal ordering of muscle activation for single-joint movements whereby proximal muscles were activated before distal muscles. Specifically, they found that the onset of shoulder muscle activity preceded not just elbow movement but also the onset of elbow muscle activity by 20–50 ms, a finding also evident at the level of single neurons in the monkey primary motor cortex (Fetz et al. 1989; Humphrey 1972; Scott 1997). Although our results are broadly consistent with this proximal to distal rule, the timing differences we found were either substantially smaller than previously reported ($<$20 ms) and/or did not reach statistical significance (Figs. 5 and 9).

One possibility is that the proximal to distal differences in recruitment timing merely reflect the conduction delays associated with neural commands propagating to more distal muscles. This simple explanation is attractive but seems unlikely

Fig. 13. Perturbation evoked movement in *experiment 4*. *A*: kinematics of the shoulder, elbow, and wrist joints are shown following a multijoint perturbation when the wrist was positioned at 60°. *B*: data for kinematics when the wrist was positioned at −40° are shown using the same format as *A*. *C*: mean shoulder and elbow joint displacement at 50 ms postperturbation is shown for *load combination 1* (see METHODS). *$P < 0.0001$, $t_{14} = -5.93$, paired *t*-test. Gray lines indicate data from individual participants. *D*: shoulder and elbow joint angles at 50 ms postperturbation are shown for *load combination 1*.
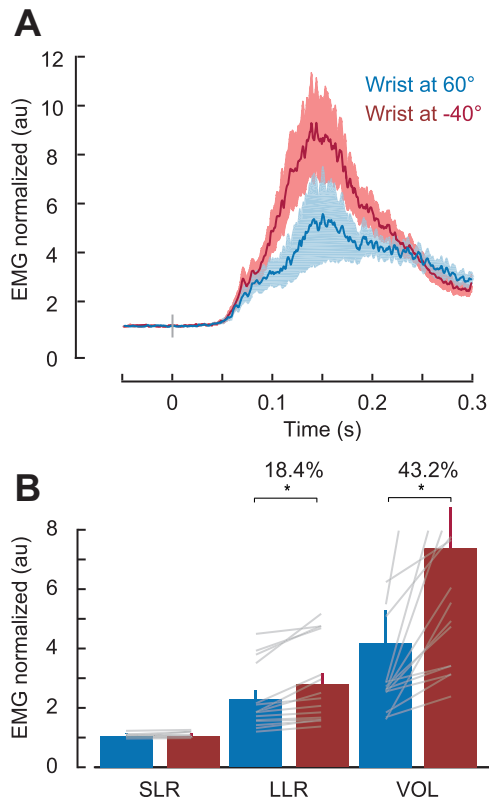
A

B

Fig. 14. Fast feedback responses in *experiment 4*. *A*: mean PEC muscle activity is shown for 2 different hand orientations for *load combination 1* (see METHODS). Data are aligned on perturbation onset. Shaded areas represent SE. *B*: bars represent the mean muscle activity in predefined epochs relative to perturbation onset: short-latency (20–50 ms), long-latency (50–100 ms), and voluntary responses (100–150 ms). Gray lines represent data from individual participants. *$P < 0.05$, reliable effects (see text).

given that such delays would account for substantially less than ~5 ms (Ingram et al. 1987; Wang et al. 1999). Moreover, it should be emphasized that our onset time estimates (and most previous studies showing similar effects) may be biased in a way that underestimates onset timing differences between distal and proximal muscles. That is, techniques that estimate muscle onset time as the time when the EMG signal reaches some arbitrary threshold relative to baseline will be biased toward earlier values for muscles showing greater activation levels, the more distal muscles in our experiments. We thus consider our estimate of onset timing differences a lower bound on how much the onset of activity in the distal muscles leads proximal muscles in our task.

It is important to note that the proximal-distal rule is not mandatory. For example, a large body of work in object manipulation has shown that grip forces used to stabilize handheld objects are modulated roughly in phase with the self-generated forces arising during arm movements with object manipulation (Danion and Sarlegna 2007; Diamond et al. 2015; Flanagan and Wing 1997; Hadjiosif and Smith 2015; Wolpert and Flanagan 2001). So why are proximal muscles activated before distal muscles in the simple reaching task used in the present experiments? Previous work has suggested that the multijoint movement is organized in a hierarchical structure with leading and subordinate joints (Dounskaia 2005). Muscles at the leading joint act to accelerate the limb as during single-joint movement, and muscles at the subordinate joint act to

regulate interaction torques and tune net torque to create the desired movement. This simplifying control structure is appealing in many respects but does not provide a clear explanation for our findings. That is, if the distal joint is the leading joint, which seems sensible given that this is the only segment with net acceleration, then according to the leading joint hypothesis, it should be activated before the proximal joint that needs to regulate interaction torques to keep the hand on target. Gribble and Ostry (1999) proposed the more general idea that a proximal to distal rule might reflect an organizational strategy for maintaining limb stability. However, from a purely mechanical perspective, there is no clear reason to preactivate proximal muscles to counter interaction torques arising from distal joint rotation. One possibility is that onset differences could reflect different force recruitment properties of muscles spanning these different joints. Indeed, previous work in monkeys reveals a relatively high abundance of fast-twitch muscle fibers in superficial elbow flexors (Singh et al. 2002), and it is the flexor condition where we see the largest and most reliable lead in shoulder muscle onset times. Although this explanation is appealing for the shoulder and elbow, it does not necessarily support a general proximal-distal rule for arm muscles. Additional work is clearly needed to establish the general validity of the proximal-distal rule and to link it to a specific mechanism.

Accounting for interaction torques during feedback control. Many studies have shown that the nervous system accounts for the limb's intersegmental dynamics during self-initiated (i.e., feedforward) control of the arm (Almeida et al. 1995; Cooke and Virji-Babul 1995; Corcos et al. 1989; Galloway and Koshland 2002; Gottlieb 1998; Gribble and Ostry 1999; Gritsenko et al. 2011; Hollerbach and Flash 1982; Koshland et al. 1991; Pigeon et al. 2003, 2013; Sainburg et al. 1995, 1999; Virji-Babul and Cooke 1995). A related series of studies has demonstrated that this capacity is also present during reflexive (i.e., feedback) control of the arm (Crevecoeur et al. 2012; Kurtzer et al. 2008, 2009, 2014, 2016; Lacquaniti and Soechting 1984, 1986a, 1986b; Pruszynski et al. 2011; Soechting and Lacquaniti 1988). For example, Soechting and Lacquaniti (1988) investigated rapid feedback responses following mechanical perturbations at the shoulder and elbow joints when both joints were free to move. They showed that feedback responses starting ~20 ms after perturbation onset (i.e., the short-latency stretch response) reflected motion at one joint, whereas those starting ~50 ms after perturbation onset (i.e., the long-latency stretch response) reflected motion at multiple joints. Kurtzer et al. (2008) further investigated this issue by applying a specific combination of mechanical perturbations at the shoulder and elbow joints that led to either *1*) the same motion at the shoulder and different motion patterns at the elbow or *2*) minimal motion at the shoulder and different motion patterns at the elbow. Their results showed that the short-latency stretch response responded only to local joint motion, whereas the long-latency stretch response accounts for the limb's intersegmental dynamics and responds to the underlying applied torques.

Our present work (*experiment 4*) tested whether feedback control of the arm accounts for the limb's intersegmental dynamics across the whole arm. We did so by applying two sets of loads to the shoulder and elbow that yielded similar motion profiles at the shoulder and elbow joints when the wrist was locked in two different configurations. As in *experiment 3*,

the applied loads were quite similar because the mass of the hand has a subtle influence on the overall mechanical properties of the arm. Nevertheless, we saw robust changes during the long-latency stretch response that were appropriate for countering the underlying applied loads with the wrist positioned in different configurations. Thus it appears that the nervous system is highly sensitive to intersegmental dynamics across the shoulder, elbow, and wrist joints during both feedforward and feedback control.

The functional similarity between feedforward and feedback control in our study lends further support to the idea that these responses engage a similar neural circuit. One likely node in this circuit is primary motor cortex. Gritsenko et al. (2011) used transcranial magnetic stimulation over the human primary motor cortex during self-initiated reaching movements toward targets that included assistive or resistive interaction torques. Their results showed that motor evoked potentials were greater for movement directions that included resistive interaction torques compared with assistive movements, suggesting that M1 indeed mediates feedforward compensation for the limb's intersegmental dynamics. Similarly, Pruszynski et al. (2011) showed that transcranial magnetic stimulation over M1 in humans can potentiate shoulder muscle responses following mechanical perturbations that cause pure elbow displacement, suggesting that M1 mediates feedback compensation for the limb's intersegmental dynamics. An important area of future research, which we are actively pursuing, is determining whether the same neurons in M1 carry these signals for feedforward and feedback control, and whether these signals reflect processing intrinsic to M1 or whether they reflect computations performed in other parts of the brain.

DISCLOSURES

No conflicts of interest, financial or otherwise, are declared by the authors.

AUTHOR CONTRIBUTIONS

R.S.M. and J.A.P. conceived and designed research; R.S.M. performed experiments; R.S.M. analyzed data; R.S.M., T.C., P.L.G., and J.A.P. interpreted results of experiments; R.S.M. prepared figures; R.S.M. and J.A.P. drafted manuscript; R.S.M., T.C., P.L.G., and J.A.P. edited and revised manuscript; R.S.M., T.C., P.L.G., and J.A.P. approved final version of manuscript.

REFERENCES

Almeida GL, Hong DA, Corcos D, Gottlieb GL. Organizing principles for voluntary movement: extending single-joint rules. *J Neurophysiol* 74: 1374–1381, 1995.

Burdet E, Osu R, Franklin DW, Milner TE, Kawato M. The central nervous system stabilizes unstable dynamics by learning optimal impedance. *Nature* 414: 446–449, 2001. doi:10.1038/35106566.

Cooke JD, Virji-Babul N. Reprogramming of muscle activation patterns at the wrist in compensation for elbow reaction torques during planar two-joint arm movements. *Exp Brain Res* 106: 177–180, 1995. doi:10.1007/BF00241366.

Corcos DM, Gottlieb GL, Agarwal GC. Organizing principles for single-joint movements. II. A speed-sensitive strategy. *J Neurophysiol* 62: 358–368, 1989.

Crevecoeur F, Kurtzer I, Scott SH. Fast corrective responses are evoked by perturbations approaching the natural variability of posture and movement tasks. *J Neurophysiol* 107: 2821–2832, 2012. doi:10.1152/jn.00849.2011.

Danion F, Sarlegna FR. Can the human brain predict the consequences of arm movement corrections when transporting an object? Hints from grip force adjustments. *J Neurosci* 27: 12839–12843, 2007. doi:10.1523/JNEUROSCI.3110-07.2007.

Debicki DB, Gribble PL. Persistence of inter-joint coupling during single-joint elbow flexions after shoulder fixation. *Exp Brain Res* 163: 252–257, 2005. doi:10.1007/s00221-005-2229-6.

Diamond JS, Nashed JY, Johansson RS, Wolpert DM, Flanagan JR. Rapid visuomotor corrective responses during transport of hand-held objects incorporate novel object dynamics. *J Neurosci* 35: 10572–10580, 2015. doi:10.1523/JNEUROSCI.1376-15.2015.

Dounskaia N. The internal model and the leading joint hypothesis: implications for control of multi-joint movements. *Exp Brain Res* 166: 1–16, 2005. doi:10.1007/s00221-005-2339-1.

Fetz EE, Cheney PD, Mewes K, Palmer S. Control of forelimb muscle activity by populations of corticomotoneuronal and rubromotoneuronal cells. *Prog Brain Res* 80: 437–449, 1989. doi:10.1016/S0079-6123(08)62241-4.

Flanagan JR, Wing AM. The role of internal models in motion planning and control: evidence from grip force adjustments during movements of hand-held loads. *J Neurosci* 17: 1519–1528, 1997.

Franklin DW, Liaw G, Milner TE, Osu R, Burdet E, Kawato M. Endpoint stiffness of the arm is directionally tuned to instability in the environment. *J Neurosci* 27: 7705–7716, 2007. doi:10.1523/JNEUROSCI.0968-07.2007.

Galloway JC, Koshland GF. General coordination of shoulder, elbow and wrist dynamics during multijoint arm movements. *Exp Brain Res* 142: 163–180, 2002. doi:10.1007/s002210100882.

Gottlieb GL. Muscle activation patterns during two types of voluntary single-joint movement. *J Neurophysiol* 80: 1860–1867, 1998.

Gribble PL, Ostry DJ. Compensation for interaction torques during single- and multijoint limb movement. *J Neurophysiol* 82: 2310–2326, 1999.

Gritsenko V, Kalaska JF, Cisek P. Descending corticospinal control of intersegmental dynamics. *J Neurosci* 31: 11968–11979, 2011. doi:10.1523/JNEUROSCI.0132-11.2011.

Hadjiosif AM, Smith MA. Flexible control of safety margins for action based on environmental variability. *J Neurosci* 35: 9106–9121, 2015. doi:10.1523/JNEUROSCI.1883-14.2015.

Hogan N. The mechanics of multi-joint posture and movement control. *Biol Cybern* 52: 315–331, 1985. doi:10.1007/BF00355754.

Hollerbach MJ, Flash T. Dynamic interactions between limb segments during planar arm movement. *Biol Cybern* 44: 67–77, 1982. doi:10.1007/BF00353957.

Humphrey DR. Relating motor cortex spike trains to measures of motor performance. *Brain Res* 40: 7–18, 1972. doi:10.1016/0006-8993(72)90099-6.

Ingram DA, Davis GR, Swash M. Motor nerve conduction velocity distributions in man: results of a new computer-based collision technique. *Electroencephalogr Clin Neurophysiol* 66: 235–243, 1987. doi:10.1016/0013-4694(87)90072-1.

Koshland GF, Hasan Z, Gerilovsky L. Activity of wrist muscles elicited during imposed or voluntary movements about the elbow joint. *J Mot Behav* 23: 91–100, 1991. doi:10.1080/00222895.1991.9942026.

Kurtzer I, Crevecoeur F, Scott SH. Fast feedback control involves two independent processes utilizing knowledge of limb dynamics. *J Neurophysiol* 111: 1631–1645, 2014. doi:10.1152/jn.00514.2013.

Kurtzer I, Meriggi J, Parikh N, Saad K. Long-latency reflexes of elbow and shoulder muscles suggest reciprocal excitation of flexors, reciprocal excitation of extensors, and reciprocal inhibition between flexors and extensors. *J Neurophysiol* 115: 2176–2190, 2016. doi:10.1152/jn.00929.2015.

Kurtzer I, Pruszynski JA, Scott SH. Long-latency responses during reaching account for the mechanical interaction between the shoulder and elbow joints. *J Neurophysiol* 102: 3004–3015, 2009. doi:10.1152/jn.00453.2009.

Kurtzer IL, Pruszynski JA, Scott SH. Long-latency reflexes of the human arm reflect an internal model of limb dynamics. *Curr Biol* 18: 449–453, 2008. doi:10.1016/j.cub.2008.02.053.

Lacquaniti F, Soechting JF. Behavior of the stretch reflex in a multi-jointed limb. *Brain Res* 311: 161–166, 1984. doi:10.1016/0006-8993(84)91411-2.

Lacquaniti F, Soechting JF. EMG responses to load perturbations of the upper limb: effect of dynamic coupling between shoulder and elbow motion. *Exp Brain Res* 61: 482–496, 1986a. doi:10.1007/BF00237573.

Lacquaniti F, Soechting JF. Responses of mono- and bi-articular muscles to load perturbations of the human arm. *Exp Brain Res* 65: 135–144, 1986b. doi:10.1007/BF00243836.

McIntyre J, Mussa-Ivaldi FA, Bizzi E. The control of stable postures in the multijoint arm. *Exp Brain Res* 110: 248–264, 1996. doi:10.1007/BF00228556.

Milner TE. Accuracy of internal dynamics models in limb movements depends on stability. *Exp Brain Res* 159: 172–184, 2004. doi:10.1007/s00221-004-1944-8.

Pigeon P, Bortolami SB, DiZio P, Lackner JR. Coordinated turn-and-reach movements. I. Anticipatory compensation for self-generated coriolis and interaction torques. *J Neurophysiol* 89: 276–289, 2003. doi:10.1152/jn.00159.2001.

Pigeon P, Dizio P, Lackner JR. Immediate compensation for variations in self-generated Coriolis torques related to body dynamics and carried objects. *J Neurophysiol* 110: 1370–1384, 2013. doi:10.1152/jn.00104.2012.

Pruszynski JA, Kurtzer I, Nashed JY, Omrani M, Brouwer B, Scott SH. Primary motor cortex underlies multi-joint integration for fast feedback control. *Nature* 478: 387–390, 2011. doi:10.1038/nature10436.

Pruszynski JA, Kurtzer I, Scott SH. Rapid motor responses are appropriately tuned to the metrics of a visuospatial task. *J Neurophysiol* 100: 224–238, 2008. doi:10.1152/jn.90262.2008.

Pruszynski JA, Scott SH. Optimal feedback control and the long-latency stretch response. *Exp Brain Res* 218: 341–359, 2012. doi:10.1007/s00221-012-3041-8.

Sainburg RL, Ghez C, Kalakanis D. Intersegmental dynamics are controlled by sequential anticipatory, error correction, and postural mechanisms. *J Neurophysiol* 81: 1045–1056, 1999.

Sainburg RL, Ghilardi MF, Poizner H, Ghez C. Control of limb dynamics in normal subjects and patients without proprioception. *J Neurophysiol* 73: 820–835, 1995.

Scott SH. Comparison of onset time and magnitude of activity for proximal arm muscles and motor cortical cells before reaching movements. *J Neurophysiol* 77: 1016–1022, 1997.

Shemmell J, Krutky MA, Perreault EJ. Stretch sensitive reflexes as an adaptive mechanism for maintaining limb stability. *Clin Neurophysiol* 121: 1680–1689, 2010. doi:10.1016/j.clinph.2010.02.166.

Singh K, Melis EH, Richmond FJ, Scott SH. Morphometry of *Macaca mulatta* forelimb. II. Fiber-type composition in shoulder and elbow muscles. *J Morphol* 251: 323–332, 2002. doi:10.1002/jmor.1092.

Soechting JF, Lacquaniti F. Quantitative evaluation of the electromyographic responses to multidirectional load perturbations of the human arm. *J Neurophysiol* 59: 1296–1313, 1988.

Virji-Babul N, Cooke JD. Influence of joint interactional effects on the coordination of planar two-joint arm movements. *Exp Brain Res* 103: 451–459, 1995. doi:10.1007/BF00241504.

Wang FC, de Pasqua V, Delwaide PJ. Age-related changes in fastest and slowest conducting axons of thenar motor units. *Muscle Nerve* 22: 1022–1029, 1999. doi:10.1002/(SICI)1097-4598(199908)22:8<1022::AID-MUS3>3.0.CO;2-F.

Weiler J, Gribble PL, Pruszynski JA. Goal-dependent modulation of the long-latency stretch response at the shoulder, elbow, and wrist. *J Neurophysiol* 114: 3242–3254, 2015. doi:10.1152/jn.00702.2015.

Weiler J, Saravanamuttu J, Gribble PL, Pruszynski JA. Coordinating long-latency stretch responses across the shoulder, elbow, and wrist during goal-directed reaching. *J Neurophysiol* 116: 2236–2249, 2016. doi:10.1152/jn.00524.2016.

Winter DA. *Biomechanics and Motor Control of Human Movement* (4th ed.). Hoboken, NJ: Wiley, 2009.

Wolpert DM, Flanagan JR. Motor prediction. *Curr Biol* 11: R729–R732, 2001. doi:10.1016/S0960-9822(01)00432-8.